Medicinal Chemistry Research (2021) 30:925–939
https://doi.org/10.1007/s00044-020-02674-6

MEDICINAL CHEMISTRY RESEARCH

ORIGINAL RESEARCH

Synthesis and in vitro evaluation of triphenylphosphonium derivatives of acetylsalicylic and salicylic acids: structure-dependent interactions with cancer cells, bacteria, and mitochondria

Olga V. Tsepaeva[1] · Taliya I. Salikhova[2] · Leysan R. Grigor'eva[3] · Denis V. Ponomaryov[3] · Trinh Dang[2] · Rezeda A. Ishkaeva[2] · Timur I. Abdullin[2] · Andrey V. Nemtarev[1,3] · Vladimir F. Mironov[1,3]

Received: 9 September 2020 / Accepted: 21 November 2020 / Published online: 21 January 2021

Abstract

Salicylic acid (SA) remains one of the most fruitful natural compounds to generate drug molecules with versatile activities. In this study, effective synthesis of SA and acetylsalicylic acid (ASA) derivatives with a carrier triphenylphoshonium (TPP) group was proposed. A series of SA and ASA conjugates linked with the TPP group via alkyl chain linker (C_3-C_{10}) was synthesized. The conjugates showed enhanced TPP-mediated cytotoxicity towards MCF-7, Caco-2, PC-3 cells in proportion to the linker length. **7e, 8e** (C_9), and **7f** (C_{10}) were the most active against the cancer cells with $IC_{50} = 0.6–1.9$ μM while were less toxic for HSF. Similarly, antibacterial (bactericidal) activity of the compounds against *S. aureus* increased with the linker elongation. The lowest MIC for SA and ASA derivatives were 4 and 1 μM, respectively. The TPP conjugates induced early linker length-dependent mitochondria depolarization and concurrent superoxide radical production in the cancer cells. The most lipophilic conjugates were found to specifically interact with ROS probe 2′,7′-dichlorofluorescin diacetate, forming mixed aggregates with the probe and inhibiting its fluorescence upon oxidation. These interactions were exploited to probe the compounds inside living cells. The results identify **7e** and **7f** as promising mitochondria-modulating and anticancer agents with increased cellular availability.

Graphical Abstract

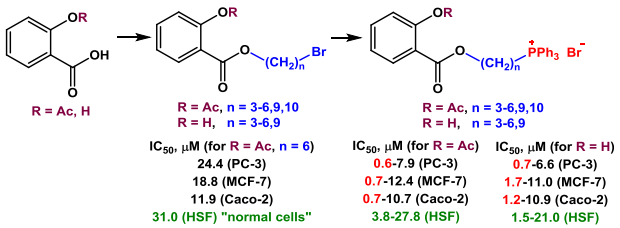

Keywords Phosphonium salts · Salicylic acid · Acetylsalicylic acid · Anticancer activity · Anticancer activity · Mitochondrial potential

Introduction

Polyhydroxybenzoates are widespread secondary metabolites in plants with vital functions [1, 2]. Among them,

These authors contributed equally: Olga V. Tsepaeva, Taliya I. Salikhova

Supplementary information The online version of this article (https://doi.org/10.1007/s00044-020-02674-6) contains supplementary material, which is available to authorized users.

✉ Andrey V. Nemtarev
a.nemtarev@mail.ru

[1] Arbuzov Institute of Organic and Physical Chemistry, FRC Kazan Scientific Center of RAS, 8 Arbuzov Str., 420088 Kazan, Russia

[2] Institute of Fundamental Medicine and Biology, Kazan (Volga Region) Federal University, 18 Kremlevskaya Str., 420008 Kazan, Russia

[3] Alexander Butlerov Institute of Chemistry, Kazan (Volga Region) Federal University, 18 Kremlevskaya Str., 420008 Kazan, Russia

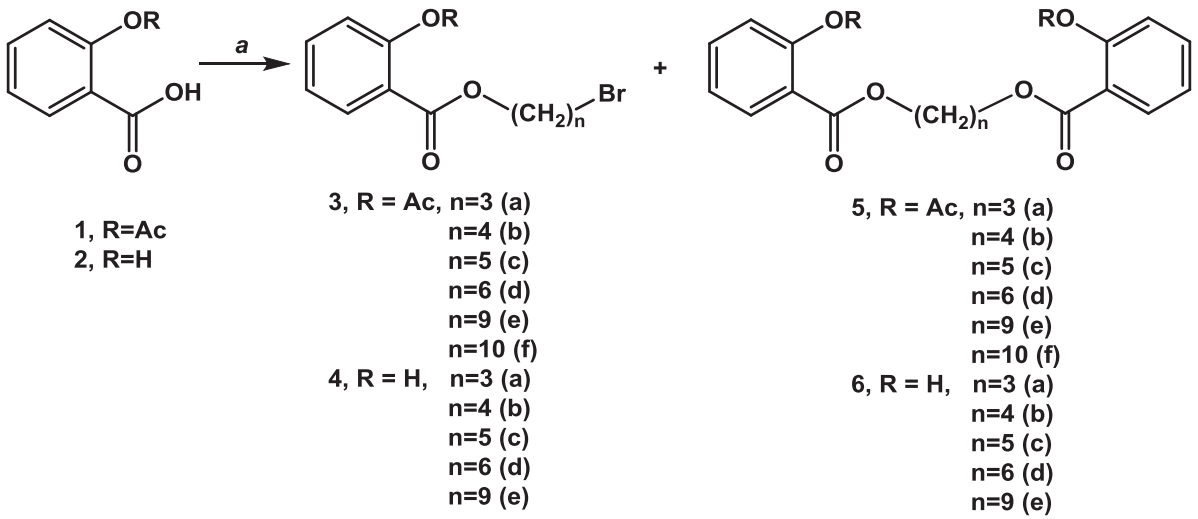

Scheme 1 Synthesis of ω-bromoalkyl esters of acetylsalicylic (**3a–f**) and salicylic (**4a–f**) acids. Reagents and conditions: **a** K_2CO_3, CH_3CN, Br $(CH_2)_nBr$

ortho-hydroxybenzoic (salicylic) acid (SA) and its esters (salicylates) are important medicinal compounds [2]. In particular, acetylsalicylic acid (ASA, aspirin) introduced over a century ago is still one of the most popular drugs with versatile prescriptions, which cover cardiovascular, inflammation and pain related diseases [3]. In recent years, polyhydroxybenzoates such as SA and gallic acids and their derivatives have attracted a great interest for preventing and treating tumor diseases [4, 5].

Several preclinical and clinical trials of ASA supported its antitumor potential [6, 7]. The mechanisms underlying antitumor action of ASA interrelate with its anti-inflammatory properties, which are generally result from the inhibition of activity of cyclooxygenases [8, 9] along with diminishing platelet activation and thrombosis involved in the cancer progression and metastasis [10, 11]. Other reported mechanisms of ASA and its active metabolite SA comprise the inhibition of IkB kinase/NF-kB pathway in vitro and in vivo [12, 13], allosteric activation of AMP-activated kinase [14], uncoupling of the respiratory chain by transporting protons across the inner mitochondrial membrane [15]. The latter activity inhibits oxidative phosphorylation, increases reactive oxygen species (ROS), thus promoting apoptosis induction [16, 17]. In addition, ASA was recently shown to induce the inhibition of acetyltransferase EP300, the suppressor of autophagy in cancer cells [18].

Owing to their therapeutic uses, polyhydroxybenzoates are considered important natural compounds to further develop drug molecules with improved pharmacokinetics, targeted properties, and new pharmacological activities [19–23]. To date, phosphonium salts and primarily triphenylphosphonium (TPP) salt were identified as one of the most powerful modifiers for small drug molecules (see reviews and references within [24–27]). Acting as a delocalized lipophilic cation, the TPP moiety effectively promotes cellular and mitochondrial accumulation of the modified compounds driven by the electrochemical gradient across biomembranes. The conjugation with TPP cation has proved to generate a range of bioactive molecules with antibacterial [28, 29], antifungal [30, 31], cyto- and neuroprotective [32], anti-inflammatory [33, 34], and anticancer [29, 35] properties.

In our group, the TPP derivatives of triterpenoids, namely, betulin, betulinic, and betulonic acids were earlier synthesized as highly-effective anticancer, antibacterial, and mitochondria-modulating compounds [29, 35]. The TPP group was shown to modulate cellular interactions and protease resistance of YRFK motif-based peptides depending on the peptide conformation and linker length; TPP-C_6-YrFK conjugate was highly resistant to enzymatic degradation [32, 36].

Existing reports on the TPP derivatives of polyhydroxybenzoates deals with comparative in vitro evaluation of decyl-TPP conjugated polyhydroxybenzoates, e.g., gallic, protocathechuic, salicylic, 2,3- and 2,5-dihydroxybenzoic acids as mitochondria-targeted compounds against breast cancer cells [27]. The alkyl gallate TPP derivatives were shown to exhibit anticancer activity via increasing the cytosolic ADP/ATP ratio, AMP level, and caspase-3 expression [37]. Furthermore, decyl-TPP gallate effectively inhibited subcutaneous adenocarcinoma tumor in mice when applied intraperitoneally in composition with doxycycline due to combined interfering effect on mitochondria [37]. Some molecular mechanisms underlying the inhibitory activity of decyl-TPP gallate on mitochondrial

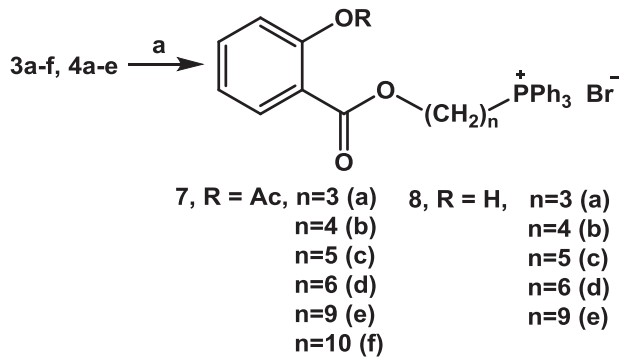

Scheme 2 Synthesis of phosphonium derivatives of acetylsalicylic (**7a–f**) and salicylic (**8a–e**) acids. Reagents and conditions: (a) PPh_3, CH_3CN, reflux

bioenergetics were recently elucidated [26]. In addition, the TPP derivatives of 2,4-dihydroxybenzoate and salicylhydroxamate [38], 4-hydroxybenzoate and 4-alkoxybenzaldehyde [39], and gallate with C_8-C_{12} alkyl linkers were [40] synthesized and proved as antitrypanosomal agents.

The current data, which are mainly focused on gallic acid derivatives, do not provide structure–bioactivity relationships for the conjugated derivatives of salicylates and TPP groups. To the best of our knowledge, the ASA-TPP conjugates have not been synthesized and evaluated to date in spite of therapeutic importance of ASA and its availability as a pharmaceutical substance. Herein, the TPP derivatives of SA and ASA with aliphatic linker of variable length (C_3–C_{10}) were synthesized and their interactions with living cells and mitochondria were for the first time compared. The conjugates with enhanced anticancer and antibacterial properties were identified. In addition, we revealed linker-dependent interactions of the conjugates with 2′,7′-dichlorofluorescin diacetate (DCFDA), which allowed to probe the compounds in solution and inside cells.

Chemistry

Results and discussion

ω-Bromoalkyl esters of SA and ASA were synthesized according to the procedure based on the reaction with 1,ω-dihalogenalkanes in acetonitrile or DMFA with an addition of potash [41]. At increased temperatures the yield of desired monoesters **3, 4** was relatively low, whereas side diesters **5, 6** amounted up to 80% of the total esterification products (Scheme 1). The diesters **5, 6** became prevailed products upon 2–4 h reaction at 90–100 °C in DMFA. Based on intense experimentation, optimal conditions for the effective synthesis of the monoesters of SA and ASA were found. They require the use of excess of 1,ω-dihalogenalkane (up to 4–6 eq.), mixed acetonitrile/DMFA solvent, and 12 h reaction at room temperature.

Synthesis of phosphonium derivatives of SA and ASA

Phosphonium derivatives of SA and ASA were obtained by the reaction of the esters **3, 4** with triphenylphosphine (PPh_3) in acetonitrile upon heating for 12–18 h (Scheme 2). The reaction progression was controlled by means of TLC and ^{31}P NMR detection of PPh_3 (δ_P 5 ppm) and the resultant TPP salts of SA and ASA (δ_P 24 ppm), which were characterized by almost quantitative yield.

Biology

Cytotoxic activity of TPP conjugates of SA and ASA

Table 1 shows IC_{50} values of the TPP conjugates **7a-f**, **8a-c**, **8e** for the cancer cell lines, namely, PC-3 (human prostate adenocarcinoma), MCF-7 (human breast adenocarcinoma), Caco-2 (human colon adenocarcinoma) cells as well as "normal" human skin fibroblasts (HSF). The SA and ASA derivatives exhibited similar to each other cytotoxicity profile, which increased by ca. ten times with the elongation of alkyl linker of the TPP group from C_3 to C_9. The compounds **7e** and **8e** were the most active against the cancer cells with IC_{50} values of 0.6–1.9 μM and 0.7–1.7 μM, respectively. Further increase of the linker length to C_{10} for the ASA derivative **7f** did not augment the cytotoxic effect. The ω-bromoalkyl derivative of ASA **3d** was 7.2–7.6 times less active against the cancer cells than the corresponding TPP conjugate **7d**, confirming the enhancing effect of the TPP cation. All TPP conjugates were significantly less toxic for HSF than for the cancer cells. For instance, such a

Table 1 IC_{50} values (μM) of acetylsalicylic and salicylic acids derivatives (MTT assay, 72 h)

Compound	PC-3	MCF-7	Caco-2	HSF
7a	7.9 ± 1.2	12.4 ± 3.8	10.7 ± 1.5	20.4 ± 0.9
7b	6.1 ± 1.7	4.9 ± 0.7	4.6 ± 0.9	27.8 ± 4.8
7c	2.0 ± 0.4	5.4 ± 1.1	3.5 ± 0.7	11.9 ± 2.3
7d	3.2 ± 0.3	2.6 ± 0.6	1.6 ± 0.3	15.8 ± 1.5
7e	0.6 ± 0.2	1.9 ± 0.1	0.7 ± 0.1	4.9 ± 0.5
7f	1.1 ± 0.3	0.7 ± 0.1	0.9 ± 0.1	3.8 ± 0.4
3d	24.4 ± 1.2	18.8 ± 1.3	11.9 ± 3.6	31.0 ± 1.4
8a	6.6 ± 0.6	11.0 ± 1.8	10.9 ± 2.9	21.0 ± 1.2
8b	2.9 ± 0.6	5.9 ± 0.9	8.1 ± 1.0	14.4 ± 2.0
8c	3.0 ± 0.7	5.0 ± 0.2	5.4 ± 0.5	10.4 ± 1.1
8e	0.7 ± 0.2	1.7 ± 0.4	1.2 ± 0.2	1.5 ± 0.2

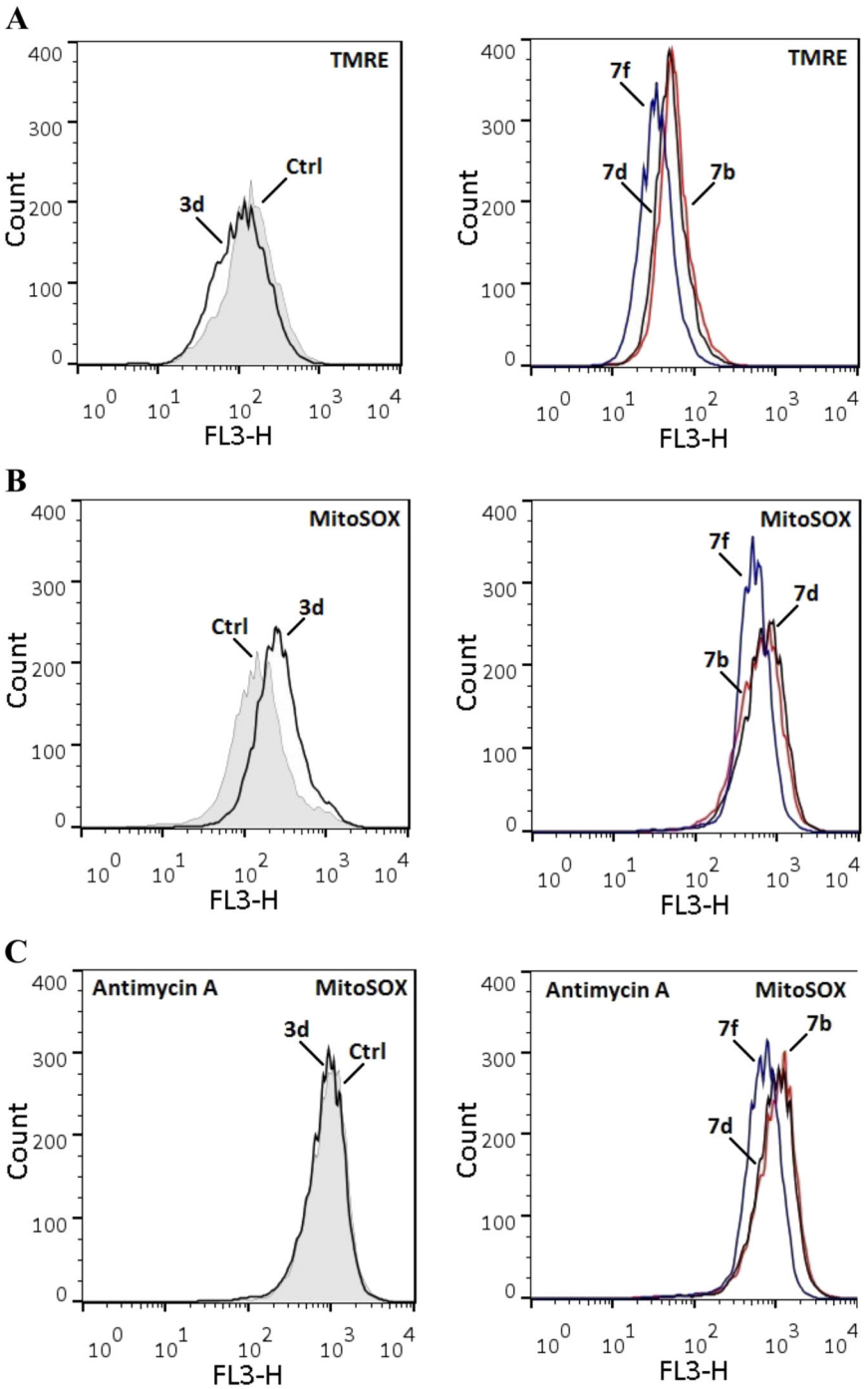

Fig. 1 Representative distribution of fluorescence of **A** TMRE and **B**, **C** MitoSOX probes in PC-3 cells treated with ASA-TPP conjugates **3d**, **7b**, **7d**, **7f** (**A**, **B**) and ASA-TPP conjugates plus antimycin A (**C**). Cells were exposed to 30 μM conjugates and 10 μM antimycin A for 1 h in HBSS. Ctrl shows untreated cells (**A**, **B**) and cells treated with antimycin A (**C**)

selectivity factor was up to 8.2 for the ASA derivative **7e** (Table 1), when compared to PC-3 cells.

The results show that the SA and ASA derivatives have enhanced anticancer activity in vitro attributed to their increased cellular/mitochondrial accumulation driven by the TPP carrier group. Such an enhancing effect of the TPP group was earlier reported for other conjugates of natural compounds [24–27,42]. Cytotoxicity of the SA and ASA derivatives was generally proportional to the linker length ($n < 10$), presumably, due to increase in their lipophilic properties. Further increase of the linker length does not seem rational due to solubility and nonspecific cytotoxicity issues. Interestingly, in contrast to the above conjugates, the TPP derivatives of triterpenoids with shorter linkers possessed higher activity in vitro [29], suggesting the role of optimal hydrophilic–lipophilic properties for each type of conjugates. The requirements for an optimal aliphatic linker to display anticancer and antiparasite activities were shown

previously for the phosphonium salts of polyhydroxybenzoates [27, 43]. The phosphonium salts of gallic acid were reported to have IC_{50} values in the range 0.4–1.6 μM for TA3/Ha, TA3-MTX-R, CCRF-CEM cancer cells [44] and to exhibit lack of toxicity for normal tissues in vivo [37]. Furthermore, their cytotoxic activity was associated with decrease in the transmembrane potential of mitochondria ($\Delta\Psi_m$) due to weak uncoupling effect [27, 37].

Cytotoxicity of mono- and di-OH benzoate decyl ester derivatives was earlier studied on breast cancer cell lines; the structure of polyhydroxybenzoate scaffold did not noticeably affect the activity of phosphonium salts [27]. Among the compounds, GATPP$^+$C10 caused time-dependent inhibition of mitochondrial bioenergetics, cell cycle arrest in G1 phase and cell death in 24 and 48 h [26].

Effect of ASA-TPP conjugates on mitochondrial potential and ROS level

To assess the interaction of TPP conjugates with mitochondria selected ASA derivatives **7b**, **7d**, **7f**, and **3d** and PC-3 cells were used. To reveal early effect on $\Delta\Psi_m$, the cells was exposed to the compounds for 1 h in HBSS at a concentration of 30 μM, which did not reduce cell viability (data not shown). According to cytofluorometry, the compounds induced decrease in $\Delta\Psi_m$ at a different extent in the order (mean channel fluorescence, a.u.): control (172) >**3d** (135)>**7b** (64)>**7d** (56)>**7f** (38). Thus, ω-bromoalkyl ester **3d** moderately affected $\Delta\Psi_m$ (by 1.3 times relative to the untreated cells), whereas the TPP conjugates induced the depolarizing effect by 2.7–4.5 times in proportion to the linker length from C_3 to C_{10} (Fig. 1A).

In addition, the level of mitochondrial ROS, i.e., superoxide radical, in the treated cells was measured with the aid of MitoSOX probe. Antimycin A was used as a model inhibitor of the mitochondrial complex III to promote ROS generation [45]. The prooxidant effect of the compounds was found to increase by 1.5–4.5 times in the order (mean channel fluorescence, a.u.): control (219) <**3d** (327) <**7f** (544) <**7b** (674) <**7d** (738) < antimycin A (981) (Fig. 1B). The compositions of antimycin A with the TPP conjugates did not enhance the ROS level in comparison with antimycin A alone.

Altogether, the results show that the ASA-TPP conjugates profoundly decrease $\Delta\Psi_m$ of PC-3 cells in comparison with the reference compound (**3d**) apparently due to increased mitochondrial accumulation, uncoupling effect on the inner membrane and concurrent overproduction of superoxide radical due to electrons leakage across the electron transport chain. The effect of TPP conjugates on $\Delta\Psi_m$ was generally proportional to the linker length (Fig. 1A). However, there was a tendency in lowering the prooxidant effect for **7f** (C_{10}) over **7d** (C_6) (Fig. 1B).

The inhibitory activity of different TPP derivatives on mitochondria functioning were previously demonstrated [46–50]. The TPP cation itself was shown to interact with and diffuse across the inner mitochondrial membrane in proportion to the electrochemical gradient allowing protons to leak into the matrix and interfering with oxidative phosphorylation [25]. The alkyl chains enhanced the activity of TPP cation so that the decyl and dodecyl TPP

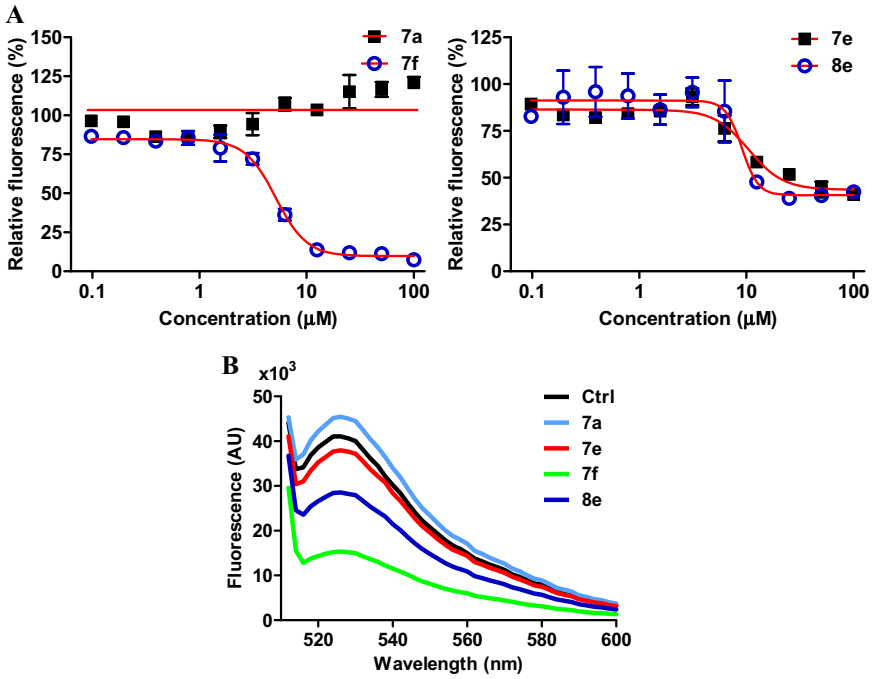

Fig. 2 Effect of selected TPP conjugates on DCFDA fluorescence induced by $CoCl_2$/H_2O_2. **A** Concentration-dependent inhibition of DCFDA oxidation in the presence of compounds. **B** Emission spectra of preoxidized DCFDA and its compositions with TPP conjugates (25 μM). 5 μM DCFDA in PBS was used. For **A** fluorescence signal (mean ± SD, $n = 3$) was presented in % relative to control oxidation reaction in the absence of conjugates (100%)

derivatives were even more powerful uncouplers than FCCP [51]. A mild uncoupling effect was established for SA (and its prodrugs) [15], which can diffuse across lipid membranes in the acidic form [42] and therefore act a as protonophor. Considering potential enzymatic lability of the ester bond in the TPP conjugates (Scheme 2), both the initial conjugates and their metabolites may be potentially responsible for mitochondria depolarizing and prooxidant effects.

Interaction of TPP conjugates with DCFDA probe

DCFDA dye, which is sensitive to intracellular ROS [52], was studied as a molecular and cellular probe for the TPP conjugates. We found that the fluorescence of DCFDA in solution induced by prooxidant $CoCl_2/H_2O_2$ system [53] was effectively inhibited in the presence of conjugates with longest linkers, i.e., **7e**, **7f**, **8e**, in the concentration range 1–100 μM unlike smaller homologs such as **7a** (Fig. 2A). **7e** and **8e** above 10 μM concentration similarly to each other induced ~50% decrease in the DCFDA signal, whereas **7f** showed the highest inhibitory effect with EC_{50} of 5.0 ± 0.6 μM (Fig. 2A). The compounds, however, did not show radical scavenging activity in the DPPH assay at a concentration up to 5 mM (data not shown).

The results show that the most lipophilic TPP conjugates interfere with the oxidation and/or fluorescence of DCFDA. Therefore, DCFDA probe was initially preoxidized and then mixed with the compounds at an effective concentration of 25 μM. Under these conditions, **8e** and **7f** noticeably quenched the fluorescence of DCFDA, whereas **7a** and **7e** only modulated the signal intensity (Fig. 2B). This indicates that the inhibition of DCFDA fluorescence (Fig. 2A) may result from the direct probe-compound interaction.

Association of the TPP conjugates with DCFDA was assessed by dynamic light scattering (DLS) technique (Table 2). The compositions produced well-defined complexes with different DLS characteristics compared with the constituents, indicating the formation of mixed aggregates. Their mean hydrodynamic diameter (HD) considerably decreased from ca. 830 to 220 nm with the linker elongation in ASA derivatives from C_3 (**7a**) to C_{10} (**7f**), along with increase in their uniformity and positive zeta potential (ζ) from ca. +6 to +40 mV (Table 2). This suggests that longer alkyl linkers, i.e., C_9/C_{10}, favor the interaction of TPP conjugates with probe molecules resulting in more compact and cationic aggregates. Even smaller and more cationic aggregates were observed in the case of SA derivative with C_9 linker (**8e**) (Table 2).

Table 2 DLS data for the mixed aggregates formed by DCFDA (50 μM) and TPP conjugates (250 μM) in aqueous solution

Compound	HD (nm)	PDI	ζ (mV)
DCFDA*	2333.7 ± 288.6	0.84 ± 0.11	–20.8 ± 0.7
7a	144.7 ± 4.8	0.42 ± 0.01	–17.2 ± 1.8
7e	672.6 ± 31.1	0.34 ± 0.06	–8.6 ± 0.2
7f	188.5 ± 24.3	0.27 ± 0.04	+10.4 ± 6.9
8e*	200.3 ± 8.4	0.31 ± 0.03	+15.6 ± 0.15
7a + DCFDA	833.3 ± 144.1	0.36 ± 0.04	+6.2 ± 0.2
7e + DCFDA	291.7 ± 2.5	0.16 ± 0.01	+36.4 ± 1.4
7f + DCFDA	220.2 ± 1.6	0.12 ± 0.01	+40.2 ± 1.6
8e + DCFDA	201.8 ± 0.2	0.08 ± 0.02	+43.4 ± 1.7

*All systems except those indicated by asterisk were of good DLS quality

Altogether, the data show direct linker-dependent interaction of the TPP conjugates with DCFDA. Such a complexation may effectively quench the probe fluorescence as observed for the compounds with C_9 and C_{10} linkers (Fig. 2). Furthermore, in compact aggregates (Table 2) DCFDA molecules could be additionally protected from the oxidation. These results reveal structure-dependent intermolecular interactions of the TPP derivatives with DCFDA, which should be considered in DCFDA based assays and also can be used to probe new TPP compounds.

Probing TPP conjugates inside cells with DCFDA

Inhibition of DCFDA fluorescence by the TPP conjugates is of practical interest to assess penetration of the compounds into living cells. To verify feasibility of such an analysis, adhered PC-3 cells were preloaded with DCFDA and subjected to oxidative stress to activate the probe. Among different oxidative agents we selected $CoCl_2$, which induces metal-mediated prooxidant reactions and ROS formation [54] as well as phenazine methosulfate (PMS), which enhances superoxide radical production via mediating O_2 reduction by NAD(P)H [55]. Both agents provided reproducible concentration-dependent increase in intracellular ROS formation, however, PMS was more effective at saturated concentrations (Fig. S92). The effect of TPP conjugates (5 and 25 μM) added to the extracellular solution on the above reactions was studied (Fig. 3).

The data demonstrate that the compounds **7e**, **7f**, and **8e**, but not **7a**, inhibited DCFDA oxidation in the cells in proportion to the concentration similarly to that observed in the cell-free assay (Fig. 2A). The fluorescence signal decreased to as low as 40% ($CoCl_2$) and 10% (PMS) of the control value (100%), indicating more effective prevention of PMS-mediated oxidation of DCFDA by the conjugates. The results suggest that sufficiently lipophilic derivatives of both ASA (**7e**, **7f**) and SA (**8e**) freely penetrate the plasma membrane (presumably due to passive diffusion), reaching effective (μM) intracellular levels to interact with DCFDA molecules and inhibit their oxidation. The elongation of alkyl linker from C_9 (**7e**) to C_{10} (**7f**) significantly augmented

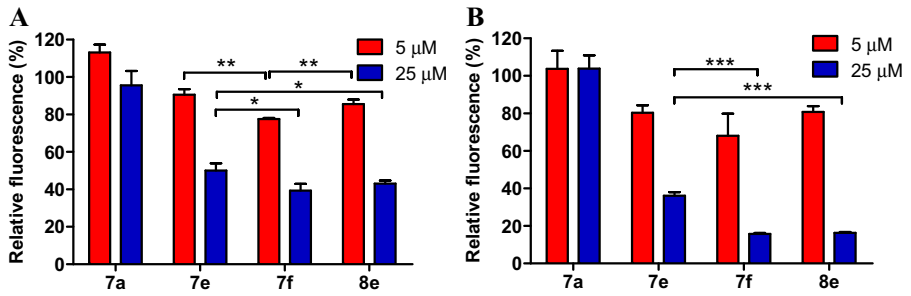

Fig. 3 Detection of TPP conjugates inside PC-3 cells using DCFDA probe. Extracellular concentration of conjugates was 5 and 25 μM; cells were pre-stained with DCFDA (20 μM) and subjected to oxidative stress by (**A**) $CoCl_2$ and (**B**) PMS. Fluorescence signal (mean ± SD, $n = 3$) was presented in % relative to control cells (100%)

the inhibitory effect, probably, due to enhanced interaction of **7f** with the DCFDA probe. Furthermore, the results show that DCFDA–TPP conjugate interaction is not inhibited in the cell interior compared with buffer solution, indicating a specific character of such a binding.

Antibacterial activity of TPP conjugates

Considering interrelationships between anticancer and antibacterial properties of TPP compounds [28, 29, 56, 57], the bacteriostatic effect of synthesized conjugates was additionally studied. Table 3 shows MIC values of the ASA and SA derivatives against *E. coli* ATCC 25922, *S. aureus* ATCC 29213. The compounds effectively prevented growth of *S. aureus* at μM concentrations but not *E. coli* in accordance with increased drug resistance of Gram-negative over Gram-positive bacteria due to specifics of cell wall structure [58, 59].

Clear increase in the bacteriostatic activity from ca. 31 to 1 μM (**7a–7f**) and 16 to 4 μM (**8a–8e**) was observed upon increase in the linker length of compounds. Both unmodified ASA and *ω*-bromoalkyl ester **3d** similarly were almost inactive (MIC = 125–500 μM), indicating that the antibacterial effect of the conjugates is determined by the TPP group. The most lipophilic ASA derivatives (**7e**, **7f**, MIC = 1 μM) were four-times more effective than the SA derivative **8e**. The linker elongation from C_9 (**7e**) to C_{10} (**7f**) did not augment the effect. Therefore, the antibacterial activity of the TPP conjugates reaches a maximum for the nonyl linker. The corresponding MIC was as low as 1 μM, which was comparable to that of existing antibiotics (Table 3).

Given that IC_{50} values of **7e** and **7f** for HSF was 4–5-times higher than the corresponding MIC (Tables 1 and 3), the compounds can be considered as potential anti-staphylococcus agents. Minimal bactericidal concentration (MBC) values of **7e** and **7f** were 2 μM (Table 3), i.e., two times higher than the corresponding MIC values, suggesting bactericidal mode of their action [60]. Similar antibacterial activity was previously reported for different organophosphorous derivatives of natural compounds, e.g., ammonium salts of dithiophosphoric acids with pyridoxine and nicotine (MIC = 10 μM) [60], TPP-pyridoxine (MIC = 5 μg/mL) [28] and TPP-triterpenoid (MIC = 2 μM) conjugates [29], carboxylate phosphabetaines derivatives (zone of inhibition = 8–28 mm) [61]. The alkyl derivatives of dimethylsubstituted and trimethylsubstituted phosphonium salts were earlier shown to possess the antibacterial activity per se, which exceeded that of the corresponding ammonium salts [62].

Table 3 MIC values (μM) of acetylsalicylic and salicylic acids derivatives (microdilution assay, 24 h)

Compound	*E. coli*	*S. aureus*
7a	125	31.25
7b	125	15.6
7c	125	15.6
7d	125	7.8
7e	125	0.98 (2)*
7f	62.5	0.98 (2)*
3d	125	250
1	250	500
8a	125	15.6
8b	125	7.8
8c	125	7.8
8e	62.5	3.9
Ciprofloxacin	1.5	1.5
Amikacin	6.7	0.8
Ceftazidime	0.9	14.3

*The values in parentheses correspond to MBC (μM)

The general mechanism of their activity may involve cell wall and membrane damage by amphiphilic organophosphorous groups. Therefore, we additionally assessed the interaction of **7e** with the bacterial surface by measuring *ζ* of the suspended bacteria (Fig. S93). The mean *ζ* of the untreated bacteria was −16.6 ± 0.4 (*E. coli*) and −19.0 ± 0.4 mV (*S. aureus*). Following brief exposition (1 h,

250 μM), **7e** was found to decrease ζ of *E. coli* by almost 10 mV (to -5.9 ± 0.3 mV, $p < 0.001$) and did not significantly affect it for *S. aureus* ($\zeta = -18.6 \pm 0.6$ mV). The results may be explained by different mechanism of **7e** interaction with the surface of Gram-positive and Gram-negative bacteria. In particular, the compounds are expected to better retain at the cell wall of *E. coli* and more readily penetrate across *S. aureus* surface.

Altogether, the data summarize linker length-dependent antibacterial properties of the TPP conjugates of SA and ASA (Table 3). Generally similar dependence was observed for cytotoxic activity of the compounds against cancer cells (Table 1). The nonyl and decyl linkers provide the maximal activity of the compounds in vitro. Further linker elongation is not advisable to design the corresponding TPP conjugates. While the effect of SA and ASA derivatives on mammalian cells did not significantly differ, latter conjugates showed somewhat higher antibacterial activity probably due to increased bacterial availability of the acetylated SA derivatives.

Conclusion

TPP conjugates of SA and ASA can be regarded as promising anticancer compounds. In this work, the productive synthesis of these conjugates was proposed. The structure of compounds was optimized in respect of their cytotoxicity for cancer and "normal" cells, mitochondria-disturbing and antibacterial activities. Specific interactions of the TPP conjugates with DCFDA, found in our study, are of interest to assess the transportation of TPP compounds into mammalian and microbial cells and coaggregation of the compounds under different conditions. The results encourage further investigation of anticancer mechanisms of the selected conjugates **7e** and **7f**.

Material and methods

All reagents and solvents were obtained from commercial sources and used without further purification. Melting points were determined on a Boetius compact heating table. The IR spectra were recorded using a Bruker Tenzor 27 spectrometer. The ^{1}H, ^{13}C, and ^{31}P NMR spectra were recorded using a Bruker Avance-400 NMR spectrometer. Chemical shifts are referenced to the residual solvent peak and reported in ppm (δ scale) and all coupling constant (J) values are given in Hz. MALDI mass spectra were acquired in the reflectron mode with Triton X-100 as a reference. A mixture of Triton X-100 solution and analyte sample (1:1 v/v) was used for internal calibration. 2,5-Dihydroxybenzoic acid (5 mg/mL in methanol) was used as a matrix. Elemental analysis was accomplished with an automated EuroVector EA3000 CHNS-O elemental analyzer (EuroVector, Italy). The progress of reactions and the purity of products were monitored by TLC on Sorbfil plates (IMID Ltd., Russian Federation). The TLC plates were visualized by treatment with phosphotungstic acid in ethanol, followed by heating to 120 °C. The targeted compounds were isolated using column chromatography on silica gel (60 A, 60–200 μm, Acros, Belgium). All solvents were dried according to standard protocols.

General procedure for the synthesis of the bromoalkane intermediates (3a–f, 4a, 4b, 4c, 4d, 4e) and dimers (5a–f, 6a, 6b, 6c, 6d, 6e)

To a solution of benzoic acid **1**, **2** (1.0 mmol) in DMF (10 mL/g), MeCN (1 mL/g), α,ω-dibromoalkane (3.0 mmol), and K_2CO_3 (1.0 mmol) were added. The reaction mixture was stirred at 50 °C for the time indicated in each case. The mixture was then poured into cold H_2O (10× volume) and extracted with $CHCl_3$ (2×15 mL each). The combined $CHCl_3$ layers were washed with H_2O (100 mL) and evaporated. The crude residue was co-evaporated with H_2O (100 mL) to remove residual DMF. The product was purified by column chromatography (petroleum ether (PE)/EtOAc; 150/10/50/50) to give compounds **3a–f**, **4a**, **4b**, **4c**, **4e** and not the 4-alkyloxy-substituted benzoic acid isomer.

3-Bromopropyl 2-(acetyloxy)benzoate, (3a)

Following the general procedure starting from 1,3-dibromopropane (0.603 g, 3 mmol). Oil (159 mg, 53%). IR (KBr) ν_{max}: 2964, 2854, 1770, 1723, 1607, 1579, 1486, 1452, 1369, 1295, 1254, 1195, 1161, 1135, 1082, 1042, 1010, 960, 917, 876, 838, 815, 795, 753, 705, 672, 651 cm^{-1}; ^{1}H NMR ($CDCl_3$, 400 MHz): δ 2.24–2.31 (m, 2H), 2.34 (s, 3H), 3.51 (t, $J = 6.5$ Hz, 2H), 4.42 (t, $J = 6.0$ Hz, 2H), 7.1 (dd, $J = 8.0$, 0.9 Hz, 1H), 7.30 (ddd, $J = 7.7$, 7.7, 1.1 Hz, 1H), 7.56 (ddd, $J = 8.0$, 7.7, 1.7 Hz, 1H), 8.0 (dd, $J = 7.8$, 1.6 Hz, 1H); anal. C, 47.74; H, 4.32; Br, 26.47%, calcd for $C_{12}H_{13}BrO_4$, C, 47.86; H, 4.35; Br, 26.53%.

4-Bromobutyl 2-(acetyloxy)benzoate, (3b)

Following the general procedure starting from 1,4-dibromobutane (0.645 g, 3 mmol). Oil (179 mg, 57%). IR (KBr) ν_{max}: 2961, 2852, 1768, 1721, 1607, 1580, 1486, 1452, 1368, 1294, 1254, 1194, 1161, 1134, 1081, 1041, 1011, 959, 916, 877, 818, 794, 753, 704, 671, 650 cm^{-1}; ^{1}H NMR ($CDCl_3$, 400 MHz): δ 1.89–1.96 (m, 2H), 1.98–2.05(m, 2H), 2.36 (s, 3H), 3.47 (t, $J = 6.5$ Hz, 2H), 4.32 (t, $J = 6.3$ Hz, 2H), 7.12 (dd, $J = 8.1$, 1.0 Hz, 1H), 7.32 (ddd, $J = 7.7$, 7.5, 1.1 Hz, 1H), 7.57 (ddd, $J = 7.5$, 7.5, 1.7 Hz), 8.01

(dd, $J = 7.8$, 1.7 Hz, 1H); anal. C 49.38; H 4.73, Br 25.36%, calcd for $C_{13}H_{15}BrO_4$, C 49.54; H 4.80, Br 25.35%.

5-Bromopentyl 2-(acetyloxy)benzoate, (3c)

Following the general procedure starting from 1,5-dibromopentane (0.690 g, 3 mmol). Oil (154 mg, 47%). IR (KBr) ν_{max}: 2944, 2867, 1770, 1720, 1607, 1579, 1485, 1452, 1368, 1294, 1261, 1195, 1161, 1134, 1082, 1041, 1010, 959, 916, 877, 856, 816, 795, 753, 705 cm^{-1}; ^1H NMR ($CDCl_3$, 400 MHz): δ 1.5–1.6 (m, 2H), 1.7–1.8 (m, 2H), 1.9-2.0 (m, 2H), 2.36 (s, 3H), 3.44 (t, $J = 6.7$ Hz, 2H), 4.3 (t, $J = 6.6$ Hz, 2H), 7.1 (dd, $J = 8.0$, 1.0 Hz, 1H), 7.3 (ddd, $J = 7.7$, 7.7, 1.2 Hz, 1H), 7.57 (ddd, $J = 8.0$, 8.0, 1.7 Hz, 1H), 8.01 (ddd, $J = 7.8$, 1.6 Hz, 1H); anal. C 51.0; H 5.18, Br 24.20%, calcd for $C_{14}H_{17}BrO_4$, C 51.08; H 5.21, Br 24.27%.

6-Bromohexyl 2-(acetyloxy)benzoate, (3d)

Following the general procedure starting from 1,6-dibromohexane (0.731 g, 3 mmol). Oil (143 mg, 42%). IR (KBr) ν_{max}: 2938, 2861, 1771, 1722, 1607, 1580, 1485, 1452, 1368, 1294, 1258, 1196, 1160, 1134, 1083, 1042, 1010, 958, 916, 876, 816, 795, 753, 705 cm^{-1}; ^1H NMR ($CDCl_3$, 400 MHz): δ 1.4–1.5 (m, 4H), 1.6–1.7 (m, 2H), 1.8–1.9 (m, 2H), 2.3 (s, 3H), 3.37 (t, $J = 6.7$ Hz, 2H), 4.25 (t, $J = 6.6$ Hz, 2H), 7.0 (dd, $J = 8.0$, 1.0 Hz, 1H), 7.27 (ddd, $J = 7.7$, 7.7, 1.1 Hz, 1H), 7.51 (ddd, $J = 8.0$, 8.0, 1.7 Hz, 1H), 8.0 (dd, $J = 7.8$, 1.5 Hz, 1H); anal. C 52.30; H 5.51, Br 23.20%, calcd for $C_{15}H_{19}BrO_4$, C 52.49; H 5.58, Br 23.28%.

9-Bromononyl 2-(acetyloxy)benzoate, (3e)

Following the general procedure starting from 1,9-dibromononane (0.572 g, 2 mmol). Oil (146 mg, 38%). IR (KBr) ν_{max}: 2930, 2856, 1772, 1722, 1608, 1579, 1485, 1452, 1368, 1294, 1259, 1195, 1160, 1134, 1082, 1041, 1010, 958, 915, 816, 753, 705 cm^{-1}; ^1H NMR ($CDCl_3$, 400 MHz): δ 1.3–1.4 (m, 10H), 1.7–1.8 (m, 2H), 1.8–1.9 (m, 2H), 2.3 (s, 3H), 3.4 (t, $J = 6.8$ Hz, 2H), 4.2 (t, $J = 6.7$ Hz, 2H), 7.1 (dd, $J = 8$, 0.9 Hz, 1H), 7.3 (ddd, $J = 7.6$, 7.6, 1.0 Hz, 1H), 7.54 (ddd, $J = 8.0$, 8.0, 1.7 Hz, 1H), 8.0 (dd, $J = 7.8$, 1.6 Hz, 1H); anal. C 55.87; H 6.51, Br 20.73%, calcd for $C_{18}H_{25}BrO_4$, C 56.11; H 6.54, Br 20.74%.

10-Bromodecyl 2-(acetyloxy)benzoate, (3f)

Following the general procedure starting from 1,10-dibromodecane (0.6 g, 2 mmol). Oil (140 mg, 35%). IR (KBr) ν_{max}: 2930, 2855, 1772, 1722, 1608, 1485, 1452, 1368, 1294, 1258, 1196, 1160, 1134, 1082, 1041, 1010, 958, 915, 816, 752, 704 cm^{-1}; ^1H NMR ($CDCl_3$, 400 MHz): δ 1.3–1.4 (m, 12H), 1.7–1.8 (m, 2H), 1.8–1.9 (m, 2H), 2.3 (s, 3H), 3.4 (t, $J = 6.8$ Hz, 2H), 4.2 (t, $J = 6.7$ Hz, 2H), 7.1 (dd, $J = 8.0$, 1.0 Hz, 1H), 7.3 (ddd, $J = 7.6$, 7.6, 1.0 Hz, 1H), 7.57 (ddd, $J = 8.0$, 8.0, 1.7 Hz, 1H), 8.0 (dd, $J = 7.8$, 1.7 Hz, 1H); anal. C 57.0; H 6.78, Br 20.0%, calcd for $C_{19}H_{27}BrO_4$, C 57.15; H 6.82, Br 20.01%.

Nonane-1,9-diyl bis(2-(acetyloxy)benzoate), (4e)

Colorless solid (121 mg, 25%); mp 67 °C. IR (KBr) ν_{max}: 2932, 2852, 1758, 1719, 1608, 1486, 1468, 1451, 1371, 1302, 1257, 1218, 1202, 1157, 1136, 1083, 1013, 956, 922, 867, 818, 799, 755, 708 cm^{-1}; ^1H NMR ($CDCl_3$, 400 MHz): δ 1.3-1.4 (m, 10H), 1.7–1.8 (m, 4H), 2.3 (s, 3H), 4.3 (t, $J =$ 6.7 Hz, 4H), 7.1 (dd, $J = 8$, 0.9 Hz, 2H), 7.3 (ddd, $J = 7.6$, 7.4, 0.7 Hz, 2H), 7.58 (ddd, $J = 8.0$, 7.6, 1.6 Hz, 2H), 8.0 (dd, $J = 7.8$, 1.6 Hz, 2H); ^{13}C NMR ($CDCl_3$, 100 MHz): δ 21.0, 25.9, 28.6, 29.2, 29.4, 65.2, 123.8, 126.0, 131.7, 133.8, 150.5, 164.5, 169.7; anal. C 66.90; H 6.60%, calcd for $C_{27}H_{32}O_8$, C 66.93; H 6.66%.

3-Bromopropyl 2-hydroxybenzoate, (4a)

Following the general procedure starting from 1,3-dibromopropane (0.603 g, 3 mmol). Oil (168 mg, 65%). IR (KBr) ν_{max}: 3190, 2966, 1677, 1614, 1585, 1485, 1467, 1396, 1328, 1301, 1251, 1214, 1159, 1137, 1092, 1032, 997, 903, 864, 801, 759, 701, 668 cm^{-1}; ^1H NMR ($CDCl_3$, 400 MHz): δ 2.35 (m, 2H), 3.53 (t, $J = 6.5$ Hz, 2H), 4.52 (t, $J = 6$ Hz, 2H), 6.90 (t, $J = 7.2$ Hz, 1H), 7.0 (d, $J = 8.3$ Hz, 1H), 7.48 (td, $J = 7.7$, 1.6 Hz, 1H), 7.84 (dd, $J = 7.9$, 1.6 Hz, 1H), 10.7 (s, 1H); anal. C, 46.24; H, 4.32; Br, 30.47%, calcd for $C_{10}H_{11}BrO_3$, C, 46.36; H, 4.28; Br, 30.84%.

4-Bromobutyl 2-hydroxybenzoate, (4b)

Following the general procedure starting from 1,4-dibromobutane (0.645 g, 3 mmol). Oil (172 mg, 63%). IR (KBr) ν_{max}: 3187, 2962, 2924, 1675, 1614, 1586, 1468, 1469, 1395, 1326, 1302, 1250, 1215, 1158, 1138, 1092, 1033, 867, 801, 758, 701 cm^{-1}; ^1H NMR ($CDCl_3$, 400 MHz): δ 1.9–2.0 (m, 4H), 3.5 (t, $J = 6.5$ Hz, 2H), 4.4 (t, $J = 6$ Hz, 2H), 6.90 (ddd, $J = 8.0$, 8.0, 1.0 Hz, 1H), 7.0 (dd, $J = 8.4$, 0.8 Hz, 1H), 7.5 (ddd, $J = 7.8$, 7.8, 1.7 Hz, 1H), 7.8 (dd, $J = 8.0$, 1.7 Hz, 1H), 10.7 (s, 1H); anal. C, 48.24; H, 4.80; Br, 28.74%, calcd for $C_{11}H_{13}BrO_3$, C, 48.37; H, 4.80; Br, 29.26%.

5-Bromopentyl 2-hydroxybenzoate, (4c)

Following the general procedure starting from 1,5-dibromopentane (0.690 g, 3 mmol). Oil (192 mg, 67%). IR (KBr)

ν_{max}: 3185, 2941, 2865, 1673, 1614, 1586, 1486, 1467, 1400, 1326, 1302, 1251, 1215, 1158, 1138, 1091, 1033, 954, 866, 801, 758, 702 cm^{-1}; ^1H NMR ($CDCl_3$, 400 MHz): δ 1.6–1.7 (m, 2H), 1.8–1.9 (m, 2H), 1.9-2.0 (m, 2H), 3.4 (t, $J = 6.7$ Hz, 2H), 4.3 (t, $J = 6.5$ Hz, 2H), 6.80 (ddd, $J = 8.0$, 8.0, 1.0 Hz, 1H), 7.0 (dd, $J = 8.3$, 0.8 Hz, 1H), 7.5 (ddd, $J = 7.8$, 7.8, 1.7 Hz, 1H), 7.8 (dd, $J = 8.0$, 1.7 Hz, 1H), 10.8 (s, 1H); anal. C, 49.75; H, 5.25; Br, 27.64%, calcd for $C_{12}H_{15}BrO_3$, C, 50.19; H, 5.27; Br, 27.83%.

6-Bromohexyl 2-hydroxybenzoate, (4d)

Following the general procedure starting from 1,6-dibromohexane (0.731 g, 3 mmol). Oil (189 mg, 63%). IR (KBr) ν_{max}: 3185, 2941, 2865, 1673, 1614, 1586, 1486, 1467, 1400, 1326, 1302, 1251, 1215, 1158, 1138, 1091, 1033, 954, 866, 801 cm^{-1} H NMR ($CDCl_3$, 400 MHz): δ 1.3–1.4 (m, 4H), 1.6–1.7 (m, 4H), 3.2 (m, Hz, 2H), 4.2 (t, $J = 6.5$ Hz, 2H), 6.73 (dd, $J = 12.5$, 7.3 Hz, 1H), 6.8 (d, $J = 8.4$ Hz, 1H), 7.3 (t, $J = 8.0$ Hz, 1H), 7.7 (d, $J = 7.9$ Hz, 1H), 10.7 (s, 1H); anal. C, 51.77; H, 5.65; Br, 26.48%, calcd for $C_{13}H_{17}BrO_3$, C, 51.84; H, 5.69; Br, 26.53%.

9-Bromononyl 2-hydroxybenzoate, (4e)

Following the general procedure starting from 1,9-dibromononane (0.572 g, 2 mmol). Oil (147 mg, 43%). IR (KBr) ν_{max}: 3181, 2930, 2856, 1674, 1614, 1586, 1486, 1467, 1396, 1326, 1302, 1251, 1214, 1187, 1158, 1138, 1091, 1033, 954, 758, 702 cm^{-1}; ^1H NMR ($CDCl_3$, 400 MHz): δ 1.3–1.4 (m, 10H), 1.7–1.9 (m, 2H), 3.4 (t, $J = 6.8$ Hz, 2H), 4.3 (t, $J = 6.6$ Hz, 2H), 6.9 (ddd, $J = 8.0$, 8.0, 1.0 Hz, 1H), 7.0 (dd, $J = 8.3$, 0.8 Hz, 1H), 7.5 (ddd, $J = 7.8$, 7.8, 1.7 Hz, 1H), 7.9 (dd, $J = 8.0$, 1.7 Hz, 1H), 10.8 (s, 1H); anal. C, 55.57; H, 6.65; Br, 23.11%, calcd for $C_{16}H_{23}BrO_3$, C, 55.99; H, 6.75; Br, 23.28%.

Nonane-1,9-diyl bis(2-hydroxylbenzoate), (6e)

Colorless solid (72 mg, 18%) mp 56 °C. IR (KBr) ν_{max}: 3143, 2964, 2925, 2856, 1678, 1614, 1587, 1488, 1468, 1399, 1325, 1302, 1252, 1215, 1194, 1157, 1134, 1092, 1033, 994, 950, 869, 815, 767, 757, 724, 695, 667 cm^{-1}; ^1H NMR ($CDCl_3$, 400 MHz): δ 1.3–1.4 (m, 10H), 1.7–1.8 (m, 4H), 4.35 (t, $J = 6.6$ Hz, 4H), 6.9 (t, $J = 7.3$ Hz, 2H), 7.0 (d, $J = 8.0$ Hz, 2H), 7.5 (td, $J = 8.6$ 1.6 Hz, 2H), 7.8 (dd, $J = 8.0$, 1.5 Hz, 2H); 10.8 (s, 2H); ^{13}C NMR ($CDCl_3$, 100 MHz): δ 25.9, 28.5, 29.1, 29.4, 65.4, 117.5, 119.0, 129.8, 135.5, 161.7, 170.2; anal. C 68.8; H 6.9%, calcd for $C_{23}H_{28}O_6$, C 68.98; H 7.05%.

General procedure for synthesis of TPP-conjugates of acetylsalicylic (7a–f) and salicylic acids (8a–e)

Triphenylphosphine (4-6 mmol) was added to the solution of bromide derivatives (**3a-f, 4a-e**) (1 mmol) in dry acetonitrile under argon, and the mixture was stirred under reflux for 6–8 h until the reaction was complete according to TLC detection. Acetonitrile was removed under reduced pressure, and the precipitate was washed with hot petroleum ether (3 × 5 mL) and dissolved in ethyl acetate. Petroleum ether (5 mL) was added to the reaction mixture. The resulting precipitate was washed with diethyl ether (3 mL) and dried in vacuo to give the pure TPP conjugate.

(3-((2-(acetyloxy)benzoyl)oxy)propyl) triphenylphosphonium bromide, (7a)

Oil; yield 92% 517 mg; IR (KBr) ν_{max}: 2964, 2854, 1770, 1723, 1607, 1579, 1486, 1452, 1369, 1295, 1254, 1195, 1161, 1135, 1082, 1042, 1010, 960, 917, 876, 815, 753, 705, 672, 651 cm^{-1}; ^1H NMR ($CDCl_3$, 400 MHz): δ 2.1 (m, 2H), 2.3 (s, 3H), 4.0 (m, 2H), 4.7 (t, $J = 5.7$ Hz, 2H), 7.0 (d, $J = 8.0$ Hz, 1H), 7.3 (t, $J = 7.4$ Hz, 1H), 7.5 (t, $J = 7.3$ Hz, 1H), 7.6–7.8 (m, 15H), 7.9 (d, 7.7 = Hz, 1H); ^{13}C NMR ($CDCl_3$, 100 MHz): 19.7 (d, $J = 52.7$ Hz), 21.3, 22.5, 64.07 (d, $J = 17.7$ Hz), 118.0 (d, $J = 86.3$ Hz), 123.1, 126.1, 130.5 (d, $J = 12.5$ Hz), 131.8, 133.8 (d, $J = 10.0$ Hz), 134.1, 135.1 (d, $J = 3.0$ Hz), 150.6, 164.2, 170.0; ^{31}P NMR ($CDCl_3$, 162 MHz): δ 24.8; anal. C, 63.09; H, 4.84; Br, 14.05; P, 5.43%, calcd for $C_{30}H_{28}BrO_4P$, C, 63.95; H, 5.01; Br, 14.18; P, 5.50%.

(4-((2-(acetyloxy)benzoyl)oxy)butyl) triphenylphosphonium bromide, (7b)

Oil; yield 90% 519 mg; IR (KBr) ν_{max}: 2866, 1764, 1717, 1606, 1485, 1438, 1368, 1295, 1255, 1196, 1161, 1113, 1085, 996, 752, 723, 690 cm^{-1}; ^1H NMR ($CDCl_3$, 400 MHz): δ 1.7–1.8 (m, 2H), 2.2–2.25 (m, 2H), 2.3 (s, 3H), 3.9–4.0 (m, 2H), 4.35 (t, $J = 6.0$ Hz, 2H), 7.1 (dd, $J =$ 8.0, 1.0 Hz, 1H), 7.27 (ddd, $J = 7.7$, 7.6, 1.0 Hz, 1H), 7.6 (ddd, $J = 7.7$, 7.7, 1.7 Hz, 1H), 7.6-7.9 (m, 16H); ^{13}C NMR ($CDCl_3$, 100 MHz): 19.6 (d, $J = 3.9$ Hz), 21.0, 22.1 (d, $J =$ 51 Hz), 28.9 (d, $J = 16.9$ Hz), 63.6, 118.0 (d, $J = 88.8$ Hz), 123.7, 125.9, 130.4 (d, $J = 12.6$ Hz), 131.4, 133.6 (d, $J =$ 10.2 Hz), 133.8, 135.0 (d, $J = 3.0$ Hz), 150.6, 164.2, 169.6; ^{31}P NMR ($CDCl_3$, 162 MHz): δ 24.3; MALDIMS, *m/z* 497 $[M–Br]^+$ (calcd *m/z* 497.19 $[M–Br]^+$ for $C_{31}H_{30}O_4P$); anal. C, 63.87; H, 5.16; Br, 13.63; P, 5.28%, calcd for $C_{31}H_{30}BrO_4P$, C, 64.48; H, 5.24; Br, 13.84; P, 5.36%.

(5-((2-(acetyloxy)benzoyl)oxy)pentyl) triphenylphosphonium bromide, (7c)

Oil; yield 93% 550 mg; IR (KBr) ν_{max}: 2907, 1766, 1718, 1607, 1588, 1485, 1451, 1439, 1368, 1295, 1257, 1197, 1162, 1114, 1083, 1041, 1011, 997, 918, 751, 724, 691 cm^{-1}; ^1H NMR ($CDCl_3$, 400 MHz): δ 1.6–1.8 (m, 6H), 2.3 (s, 3H), 3.8–3.9 (m, 2H), 4.2 (t, $J = 6.0$ Hz, 2H), 7.0 (dd, $J = 8.0$, 0.9 Hz, 1H), 7.29 (ddd, $J = 7.6$, 7.6, 1.0 Hz, 1H), 7.54 (ddd, $J = 7.5$, 7.9, 1.7 Hz, 1H), 7.6-7.9 (m, 15H), 7.95 (dd, $J = 8.0$, 0.9 Hz, 1H); ^{13}C NMR ($CDCl_3$, 100 MHz): 21.1, 22.2 (d, $J = 3.8$ Hz), 22.8 (d, $J = 50.3$ Hz), 26.8 (d, $J = 16.2$ Hz), 28.1, 64.5, 118.2 (d, $J = 86.0$ Hz), 123.5, 126.7, 130.5 (d, $J = 12.5$ Hz), 131.7, 133.6 (d, $J = 10.0$ Hz), 133.8, 135.0 (d, $J = 3.0$ Hz), 150.6, 164.3, 169.6; ^{31}P NMR ($CDCl_3$, 162 MHz): δ 24.5; MALDIMS, *m/z* 511 $[M–Br]^+$ (calcd *m/z* 511.58 $[M–Br]^+$ for $C_{32}H_{32}O_4P$); anal. C, 64.79; H, 5.31; Br, 13.41; P, 5.18%, calcd for $C_{32}H_{32}BrO_4P$, C, 64.98; H, 5.45; Br, 13.51; P, 5.24%.

(6-((2-(acetyloxy)benzoyl)oxy)hexyl) triphenylphosphonium bromide, (7d)

Oil; yield 91% 550 mg IR (KBr) ν_{max}: 2936, 2863, 1767, 1718, 1607, 1588, 1485, 1451, 1439, 1368, 1295, 1260, 1197, 1161, 1114, 1082, 1042, 997, 922, 751, 725, 692 cm^{-1}; ^1H NMR ($CDCl_3$, 400 MHz): δ 1.4 (m, 2H), 1.6–1.7 (m, 6H), 2.3 (s, 3H), 3.7–3.8 (m, 2H), 4.2 (t, $J = 6.4$ Hz, 2H), 7.0 (d, $J = 8.0$ Hz, 1H), 7.3 (m, 1H), 7.5 (t, $J = 8.4$ Hz, 1H), 7.6–7.8 (m, 15H), 7.9 (d, $J = 7.8$ Hz, 1H); ^{13}C NMR ($CDCl_3$, 100 MHz): 21.07, 22.6, 22.75 (d, $J = 50.2$ Hz), 25.5, 28.3, 29.8 (d, $J = 15.7$ Hz), 64.9, 118.3 (d, $J = 85.8$ Hz), 123.4, 126.0, 130.5 (d, $J = 12.1$ Hz), 131.7, 133.6 (d, $J = 10.0$ Hz), 133.7, 135.0 (d, $J = 3.0$ Hz), 150.6, 164.4, 169.6; ^{31}P NMR ($CDCl_3$, 162 MHz): δ 24.8; MALDIMS, *m/z* 525 $[M–Br]^+$ (calcd *m/z* 525.6 $[M–Br]^+$ for $C_{33}H_{34}O_4P$); anal. C, 65.28; H, 5.42; Br, 13.05; P, 5.18%, calcd for $C_{33}H_{34}BrO_4P$, C, 65.46; H, 5.66; Br, 13.20; P, 5.00%.

(9-((2-(acetyloxy)benzoyl)oxy)nonyl) triphenylphosphonium bromide, (7e)

Oil; yield 87% 562 mg IR (KBr) ν_{max}: 2928, 2857, 1767, 1719, 1670, 1608, 1587, 1485, 1438, 1368, 1296, 1251, 1197, 1159, 1114, 1084, 997, 922, 918, 750, 723, 691 cm^{-1}; ^1H NMR ($CDCl_3$, 400 MHz): δ 1.2–1.3 (m, 8H), 1.6–1.7 (m, 6H), 2.3 (s, 3H), 3.75 (m, 2H), 4.2 (t, $J = 6.7$ Hz, 2H), 7.0 (dd, $J = 8.0$, 0.9 Hz, 1H), 7.3 (ddd, $J = 7.8$, 7.7, 0.7 Hz 1H), 7.5 (ddd, $J = 8.0$, 8.0, 1.7 Hz, 1H), 7.6-7.8 (m, 15H), 8.0 (dd, $J = 7.9$, 1.6 Hz, 1H); ^{13}C NMR ($CDCl_3$, 100 MHz): 18.5, 20.1, 20.3 (d, $J = 48$ Hz), 23.3, 26.0, 26.5, 26.5, 27.8 (d, $J = 15.5$ Hz), 28.4, 62.7, 115.9 (d, $J = 85.8$ Hz), 121.0, 121.2, 123.5, 128.0 (d, $J = 12.5$ Hz), 129.2, 131.1 (d, $J = 10.0$ Hz), 131.2, 132.4 (d, $J = 2.7$ Hz), 148.1, 162.0, 167.1; ^{31}P NMR ($CDCl_3$, 162 MHz): δ 24.3; MALDIMS, *m/z* 567 $[M–Br]^+$ (calcd *m/z* 567.69 $[M–Br]^+$ for $C_{36}H_{40}O_4P$); anal. C, 66.58; H, 6.07; Br, 12.19; P, 4.62%, calcd for $C_{36}H_{40}BrO_4P$, C, 66.77; H, 6.23; Br, 12.34; P, 4.78%.

(10-((2-(acetyloxy)benzoyl)oxy)decyll) triphenylphosphonium bromide, (7f)

Oil; yield 85% 561 mg IR (KBr) ν_{max}: 3392, 2928, 2856, 1768(C=O), 1719, 1606, 1587, 1485, 1438, 1368, 1294, 1258, 1196, 1161, 1114, 1082, 1041, 1010, 997, 918, 794, 752, 724, 692 cm^{-1}; ^1H NMR ($CDCl_3$, 400 MHz): δ 1.2–1.3 (m, 10H), 1.6–1.7 (m, 6H), 2.3 (s, 3H), 3.73 (m, 2H), 4.2 (t, $J = 6.7$ Hz, 2H), 7.0 (dd, $J = 8.0$, 0.9 Hz, 1H), 7.3 (ddd, $J = 7.8$, 7.7, 0.7 Hz 1H), 7.5 (ddd, $J = 8.0$, 8.0, 1.7 Hz, 1H), 7.6–7.8 (m, 15H), 7.9 (dd, $J = 7.9$, 1.6 Hz, 1H); ^{13}C NMR ($CDCl_3$, 100 MHz): 21.0, 22.5 (d, $J = 52.5$ Hz), 22.7, 25.8, 28.6, 29.1, 29.3, 30.3 (d, $J = 15.3$ Hz), 65.2, 118.4 (d, $J = 85.7$ Hz), 123.5, 123.7, 126.0, 130.5 (d, $J = 12.4$ Hz), 131.7, 133.7 (d, $J = 9.4$ Hz), 135.0, 135.0, 150.6, 164.5, 169.6; ^{31}P NMR ($CDCl_3$, 162 MHz): δ 24.9; anal. C, 68.93; H, 6.27; Br, 11.56; P, 4.59%, calcd for $C_{37}H_{42}BrO_4P$, C, 67.17; H, 6.40; Br, 12.08; P, 4.68%.

(3-((2-hydroxybenzoyl)oxy)propyl) triphenylphosphonium bromide, (8a)

Oil; yield 91% 474 mg; IR (KBr) ν_{max}: 3190, 2966, 1677, 1614, 1585, 1485, 1467, 1396, 1328, 1301, 1251, 1214, 1159, 1137, 1092, 1032, 997, 903, 864, 801, 759, 701, 668 cm^{-1}; ^1H NMR ($CDCl_3$, 400 MHz): δ 2.1 (m, 2H), 4.1 (m, 2H), 4.7 (t, $J = 6.2$ Hz, 2H), 6.8 (td, $J = 8.0$, 1.0 Hz, 1H), 6.9 (dd, $J = 8.3$, 0.6 Hz 1H), 7.4 (ddd, $J = 7.8$, 7.7, 1.7 Hz, 1H), 7.6–7.8 (m, 16H), 10.5 (s, 1H); ^{13}C NMR ($CDCl_3$, 100 MHz): 19.8 (d, $J = 53.0$ Hz), 22.2 (d, $J = 3.1$ Hz), 64.3 (d, $J = 17.8$ Hz), 112.0, 117.5, 118.0 (d, $J = 86.3$ Hz), 119.3, 129.9, 130.6 (d, $J = 12.6$ Hz), 133.6 (d, $J = 10.6$ Hz), 135.2 (d, $J = 3.3$ Hz), 135.9, 161.6, 169.7; ^{31}P NMR ($CDCl_3$, 162 MHz): δ 26.0; MALDIMS, *m/z* 441 $[M–Br]^+$ (calcd *m/z* 441.16 $[M–Br]^+$ for $C_{28}H_{26}O_3P$); anal. C, 64.37; H, 4.89; Br, 15.09; P, 5.82%, calcd for $C_{28}H_{26}BrO_3P$, C, 64.50; H, 5.03; Br, 15.33; P, 5.94%.

(4-((2-hydroxybenzoyl)oxy)butyl) triphenylphosphonium bromide, (8b)

Oil; yield 92% 492 mg; IR (KBr) ν_{max}: 3353, 1664, 1610, 1484, 1439, 1396, 1328, 1298, 1248, 1222, 1159, 1113, 771, 751, 723, 691 cm^{-1}; ^1H NMR ($CDCl_3$, 400 MHz): δ 1.7–1.8 (m, 2H), 2.1-2.3 (m, 2H), 3.9–4.0 (m, 2H), 4.4 (t,

$J = 6.0$ Hz, 2H), 6.8 (ddd, $J = 7.5$, 7.6, 1.0 Hz, 1H), 6.9 (dd, $J = 8.3$, 0.6 Hz 1H), 7.4 (ddd, $J = 7.3$, 7.2, 1.7 Hz, 1H), 7.6 (dd, $J = 8.0$, 1.6 Hz, 1H), 7.6–7.9 (m, 15H), 10.6 (s, 1H); ^{13}C NMR ($CDCl_3$, 100 MHz): 19.1 (d, $J = 3.8$ Hz), 22.1 (d, $J = 50.8$ Hz), 28.9 (d, $J = 16.9$ Hz), 63.9, 112.2, 117.5, 118.5 (d, $J = 86.0$ Hz), 119.1, 129.7, 130.5 (d, $J = 12.5$ Hz), 133.6 (d, $J = 10.0$ Hz), 135.0 (d, $J = 3.0$ Hz), 135.7, 161.5, 169.9; ^{31}P NMR ($CDCl_3$, 162 MHz): δ 24.6; MALDIMS, m/z 455 $[M–Br]^+$ (calcd m/z 455.52 $[M–Br]^+$ for $C_{29}H_{28}O_3P$); anal. C, 64.91; H, 5.13; Br, 14.83; P, 5.69%, calcd for $C_{29}H_{28}BrO_3P$, C, 65.06; H, 5.27; Br, 14.92; P, 5.78%.

(5-((2-hydroxybenzoyl)oxy)pentyl) triphenylphosphonium bromide, (8c)

Oil; yield 90% 494 mg; IR (KBr) ν_{max}: 3185, 2941, 2865, 1673, 1614, 1586, 1486, 1400, 1326, 1302, 1251, 1215, 1158, 1138, 1090, 1033, 954, 866, 801, 758, 731, 702, 667 cm^{-1}; ^{1}H NMR ($CDCl_3$, 400 MHz): δ 1.7 (m, 2H), 1.8 (m, 4H), 3.9–4.0 (m, 2H), 4.3 (t, $J = 6.0$ Hz, 2H), 6.8 (ddd, $J = 8.0$, 8.0, 1.0 Hz, 1H), 6.9 (dd, $J = 8.3$, 0.6 Hz, 1H), 7.4 (ddd, $J = 7.8$, 7.8, 1.7 Hz, 1H), 7.6 (dd, $J = 8.0$, 1.6 Hz, 1H), 7.4–7.9 (m, 15H), 10.7 (s, 1H); ^{13}C NMR ($CDCl_3$, 100 MHz): 22.3, 22.9 (d, $J = 50.0$ Hz), 26.8 (d, $J = 16.1$ Hz), 28.1, 64.8, 112.5, 117.4, 118.8 (d, $J = 86.0$ Hz), 119.2, 129.9, 130.5 (d, $J = 12.5$ Hz), 133.8 (d, $J = 10.0$ Hz), 135.0 (d, $J = 3.0$ Hz), 135.6, 161.6, 170.1; ^{31}P NMR ($CDCl_3$, 162 MHz): δ 24.6; MALDIMS, m/z 469.0 $[M–Br]^+$ (calcd m/z 469.54 $[M–Br]^+$ for $C_{30}H_{30}O_3P$); anal. C, 65.39; H, 5.42; Br, 14.45; P, 5.58%, calcd for $C_{30}H_{30}BrO_3P$, C, 65.58; H, 5.50; Br, 14.54; P, 5.64%.

(6-((2-hydroxybenzoyl)oxy)hexyl) triphenylphosphonium bromide, (8d)

Colorless solid (462 mg, 82%); mp 132–133 °C; IR (KBr) ν_{max}: 3437, 2936, 2864, 2798, 1672, 1612, 1587, 1484, 1466, 1439, 1394, 1324, 1298, 1252, 1215, 1197, 1159, 1134, 1112, 1089, 993, 950, 889, 868, 748, 722, 690 cm^{-1}; ^{1}H NMR ($CDCl_3$, 400 MHz): δ 1.4–1.5 (m, 2H), 1.6–1.7 (m, 2H), 1.7–1.8 (m, 4H), 3.8 (m, 2H), 4.3 (t, $J = 6.4$ Hz, 2H), 6.9 (t, $J = 7.6$ Hz, 1H), 7.0 (d, $J = 8.3$ Hz, 1H), 7.4 (t, $J = 7.4$ Hz, 1H), 7.7–7.8 (m, 16H), 10.8 (s, 1H); ^{13}C NMR ($CDCl_3$, 100 MHz): 22.17, 23.1 (d, $J = 50.0$ Hz), 25.2, 27.8, 29.6 (d, $J = 16.0$ Hz), 64.9, 112.0, 116.9, 117.7 (d, $J = 85.8$ Hz), 118.9, 129.6, 130.3 (d, $J = 12.5$ Hz), 133.3 (d, $J = 9.2$ Hz), 134.8, 135.4, 161.0, 169.8; ^{31}P NMR ($CDCl_3$, 162 MHz): δ 24.1; anal. C, 65.92; H, 5.64; Br, 14.03; P, 5.41%, calcd for $C_{31}H_{32}BrO_3P$, C, 66.08; H, 5.72; Br, 14.18; P, 5.50%.

(9-((2-hydroxybenzoyl)oxy)nonyl) triphenylphosphonium bromide, (8e)

Oil; yield 87% 526 mg; IR (KBr) ν_{max}: 3386, 2927, 2856, 1670, 1613, 1587, 1485, 1466, 1438, 1397, 1327, 1300, 1249, 1216, 1159, 1114, 1091, 1031, 996, 751, 723, 691 cm^{-1}; ^{1}H NMR ($CDCl_3$, 400 MHz): δ 1.2–1.3 (m, 10H), 1.6-1.7 (m, 4H), 3.7 (m, 2H), 4.3 (t, $J = 6.6$ Hz, 2H), 6.8 (dd, $J = 7.8$, 7.3, Hz, 1H), 6.9 (dd, $J = 8.3$, 0.6 Hz, 1H), 7.4 (dd, $J = 7.2$, 7.2, Hz, 1H), 7.6–7.8 (m, 16H), 10.7 (s, 1H); ^{13}C NMR ($CDCl_3$, 100 MHz): 22.6, 23.0 (d, $J = 50.0$ Hz), 25.8, 28.4, 29.0, 30.3 (d, $J = 15.5$ Hz) 65.4, 112.6, 117.4, 118.3 (d, $J = 85.8$ Hz), 119.1, 129.9, 130.5 (d, $J = 12.5$ Hz),133.6 (d, $J = 10.0$ Hz), 135.0 (d, $J = 3.0$ Hz), 135.5, 161.65 170.2; ^{31}P NMR ($CDCl_3$, 162 MHz): δ 25.3; MALDIMS, m/z 525 $[M–Br]^+$ (calcd m/z 525.65 $[M–Br]^+$ for $C_{34}H_{38}O_3P$); anal. C, 67.32; H, 6.21; Br, 13.08; P, 4.99%, calcd for $C_{34}H_{38}BrO_3P$, C, 67.44; H, 6.33; Br, 13.20; P, 5.11%.

Biological assay

2′,7′-dichlorofluorescin diacetate (DCFDA), 3-(4,5-dimethylthiazol-2-yl)-2,5-diphenyltetrazolium bromide (MTT), 2,2′-diphenyl-1-picrylhydrazyl (DPPH), tetramethylrhodamine ethyl ester perchlorate (TMRE), antimycin A, phenazine methosulfate (PMS) were purchased from Sigma-Aldrich. MitoSOX Red Mitochondrial Superoxide Indicator was purchased from ThermoFisher Scientific. Milli-Q grade water (Milli-Q Advantage A10, Merck Millipore) was used to prepare buffers and solutions. Materials for cell culturing were obtained from PanEco company (Russia).

MCF-7, PC-3, and Caco-2 cancer cell lines (ATCC) were used. The cells were cultured aseptically in DMEM containing 10% fetal bovine serum (FBS), 2 mM L-glutamine, 100 U/mL penicillin and 100 µg/mL streptomycin at 37 °C in humidified air atmosphere with 5% CO_2. Human skin fibroblasts (HSF) were isolated as described earlier [35]. HSF were cultured under the same conditions but in α-MEM with 10% FBS.

Cytotoxicity study

Cytotoxic activity of the compounds was evaluated by means of the MTT proliferation assay as detailed previously [35] using an Infinite 200 PRO microplate analyzer (TECAN). Stock solutions of the compounds were prepared in DMSO and re-dissolved in HBSS; the cytotoxicity of residual amounts of DMSO was verified. The cells were cultured in the presence of compounds in the concentration range from 48.9 nM to 100 µM for 72 h. Cell viability was presented relative to control cells grown without compounds (100% viability). Half-maximal inhibitory concentrations (IC_{50})

were calculated from concentration–viability relationships using OriginPro software.

DPPH and DCFDA assays

The measurements were performed in a 96-well plate on an Infinite 200 PRO microplate analyzer. In the DPPH-assay serially diluted compounds were mixed with 0.25 mM DPPH in PBS supplemented with Triton X100 (8 mg/mL) followed by the colorimetric detection of the unreacted DPPH at $\lambda = 515$ nm [53]. The Fenton system used to oxidize DCFDA (5 μM) fluorescent probe comprised 0.23 mM $CoCl_2$ and 22 mM H_2O_2 in PBS. The fluorescence intensity of DCFDA upon oxidation was detected at $\lambda_{ex} =$ 488 nm and $\lambda_{em} = 535$ nm [53]. The effect of compounds on the DCFDA was evaluated in the concentration range 0.1–100 μM signal.

For cell based DCFDA assay pre-grown PC-3 cells were stained with 20 μM DCFDA for 30 min, washed with PBS and subjected to the oxidative stress by addition of $CoCl_2$ (0.002–4 mM) or PMS (0.003–0.1 mM) in PBS followed by the detection of bottom fluorescence at $\lambda_{ex}/\lambda_{em} = 488/$ 535 nm. The compounds were added to the extracellular solution at a concentration of 25 μM.

Analysis of mitochondrial potential and ROS

The analysis was performed on a BD FACSCalibur flow cytometer (BD Biosciences). Briefly, PC-3 cells were collected with the aid of trypsin-EDTA dissociation solution, washed with and suspended in HBSS at a density of 10^6 cells/mL. Then the cells were mixed with the compounds (30 μM) and incubated for 1 h at 37 °C in the CO_2-incubator. The treated cells were stained with 0.1 μM TMRE for 20 min at 37 °C to analyze transmembrane potential of mitochondria. To evaluate mitochondrial ROS 5 μM MitoSOX was added to the cell suspension and incubated for 20 min at 37 °C in the CO_2-incubator. The prestained cells were diluted to a density of 3×10^5 cells/mL, then mixed with the synthesized compounds (30 μM) and/or antymicin A (10 μM) and incubated at 37 °C for 1 h. Cell viability was additionally verified by bright-filed microscopy and the MTT assay in parallel samples.

Study of antibacterial activity

Escherichia coli and *Staphylococcus aureus* ATCC 29213 were used. Bacteriostatic activity was studied by the microdilution method in Mueller–Hinton broth [60]. Sterile serially diluted compounds (250–0.5 μM) were mixed with the bacterial inoculum in 96-well plates and incubated for 24 h at 37 °C under moderate shaking. Bacterial growth was analyzed visually in three parallel wells by appearance of turbidity/precipitate and, in addition, by the change in color of phenol red indicator (18 μg/mL). Minimal inhibitory concentration (MIC) values were determined as minimal concentrations of a compound prevented bacteria growth. To determine minimal bactericidal concentration (MBC), an aliquot of the treated bacterial culture was transferred onto Mueller–Hinton agar. MBC was the minimal concentration at which bacterial colonies were not detected.

Dynamic light scattering (DLS) analysis

The HD, particle dispersion index (PDI), and ζ of molecular aggregates of DCFDA (50 μM), the compounds (250 μM) and their compositions in milliQ water were measured with the aid of DLS technique on a Zetasizer NanoZS analyzer (Malvern Instruments). To determine ζ of bacteria, the night culture was diluted with PBS at 10^9 CFU/mL and mixed with a compound (1 mM) or PBS (control) followed by incubation for 1 h at 37 °C upon shaking. The treated bacteria were collected by centrifugation, resuspended in 50 mM HEPES buffer (pH = 7) and subjected to the analysis.

Statistical analysis

Quantitative data were presented as mean ± SD ($n \geq 3$). The normality of the data distribution and the significance of differences were assessed using GraphPad Prism 5.0 software (Student's t test, $p < 0.05$).

Acknowledgements This work was supported by the Ministry of Education and Science of the Russian Federation (subsidies allocated to FRC Kazan Scientific Center of RAS and Kazan Federal University for the state assignments in the sphere of scientific activities (0671-2020-0063)), the Russian Foundation for Basic Research (grant no. 20-33-70194), and also performed according to the Russian Government Program of Competitive Growth of Kazan Federal University. RI acknowledges RFBR project No 19-34-90139 (analysis of oxidative stress in cell monolayers). The authors gratefully acknowledge the CSF-SAC FRC KSC RAS and Interdisciplinary Centre for Shared Use of Kazan Federal University.

Compliance with ethical standards

Conflict of interest The authors declare that they have no conflict of interest.

Publisher's note Springer Nature remains neutral with regard to jurisdictional claims in published maps and institutional affiliations.

References

1. Hayat S, Ahmad A. Salicylic acid—a plant hormone. Netherlands: Springer; 2007.
2. Duthie GG, Wood AD. Natural salicylates: foods, functions and disease prevention. Food Funct. 2011;2:515–20. https://doi.org/10.1039/C1FO10128E.

3. Awtry EH, Loscalzo J. Aspirin. Circulation. 2000;101:1206–18. https://doi.org/10.1161/01.cir.101.10.1206.
4. Sun G, Zhang S, Xie Y, Zhang Z, Zhao W. Gallic acid as a selective anticancer agent that induces apoptosis in SMMC-7721 human hepatocellular carcinoma cells. Oncol Lett. 2016;11:150–8. https://doi.org/10.3892/ol.2015.3845.
5. Ghasemzadeh A, Jaafar HZE, Karimi E. Involvement of salicylic acid on antioxidant and anticancer properties, anthocyanin production and chalcone synthase activity in ginger (Zingiber officinale Roscoe) varieties. Int J Mol Sci. 2012;13:14828–44. https://doi.org/10.3390/ijms131114828.
6. Holmes MD, Chen WY, Li L, Hertzmark E, Spiegelman D, Hankinson SE. Aspirin intake and survival after breast cancer. J Clin Oncol. 2010;28:1467–72. https://doi.org/10.1200/JCO.2009.22.7918.
7. Chan AT, Ogino S, Fuchs CS. Aspirin use and survival after diagnosis of colorectal cancer. JAMA. 2009;302:649–58. https://doi.org/10.1001/jama.2009.1112.
8. Thun MJ, Henley SJ, Patrono C. Nonsteroidal anti-inflammatory drugs as anticancer agents: mechanistic, pharmacologic, and clinical issues. J Natl Cancer Inst. 2002;94:252–66. https://doi.org/10.1093/jnci/94.4.252.
9. Roth GJ, Majerus PW. The mechanism of the effect of aspirin on human platelets. I. Acetylation of a particulate fraction protein. J Clin Investig. 1975;56:624–32. https://doi.org/10.1172/JCI108132.
10. Kuznetsov HS, Marsh T, Markens BA, Castaño Z, Greene-Colozzi A, Hay SA, et al. Identification of luminal breast cancers that establish a tumor-supportive macroenvironment defined by proangiogenic platelets and bone marrow–derived cells. Cancer Discov. 2012;2:1150–65. https://doi.org/10.1158/2159-8290.CD-12-0216.
11. Coppinger JA, O'Connor R, Wynne K, Flanagan M, Sullivan M, Maguire PB, et al. Moderation of the platelet releasate response by aspirin. Blood. 2007;109:4786–92. https://doi.org/10.1182/blood-2006-07-038539.
12. McCarty MF, Block KI. Preadministration of high-dose salicylates, suppressors of NF-κB activation, may increase the chemosensitivity of many cancers: an example of proapoptotic signal modulation therapy. Integr Cancer Ther. 2006;5:252–68. https://doi.org/10.1177/1534735406291499.
13. Kopp E, Ghosh S. Inhibition of NF-kappa B by sodium salicylate and aspirin. Science. 1994;265:956–9. https://doi.org/10.1126/science.8052854.
14. Hawley SA, Fullerton MD, Ross FA, Schertzer JD, Chevtzoff C, Walker KJ, et al. The ancient drug salicylate directly activates AMP-activated protein kinase. Science. 2012;336:918–22. https://doi.org/10.1126/science.1215327.
15. Petrescu I, Tarba C. Uncoupling effects of diclofenac and aspirin in the perfused liver and isolated hepatic mitochondria of rat. Biochim Biophys Acta. 1997;1318:385–94. https://doi.org/10.1016/s0005-2728(96)00109-0.
16. Dikshit P, Chatterjee M, Goswami A, Mishra A, Jana NR. Aspirin induces apoptosis through the inhibition of proteasome function. J Biol Chem. 2006;281:29228–35. https://doi.org/10.1074/jbc.M602629200.
17. Raza H, John A, Benedict S. Acetylsalicylic acid-induced oxidative stress, cell cycle arrest, apoptosis and mitochondrial dysfunction in human hepatoma HepG2 cells. Eur J Pharmacol. 2011;668:15–24. https://doi.org/10.1016/j.ejphar.2011.06.016.
18. Castoldi F, Pietrocola F, Maiuri MC, Kroemer G. Aspirin induces autophagy via inhibition of the acetyltransferase EP300. Oncotarget. 2018;9:24574-5. https://doi.org/10.18632/oncotarget.25364.
19. Ekinci D, Şentürk M, Küfrevioğlu Öİ. Salicylic acid derivatives: synthesis, features and usage as therapeutic tools. Exp Opin Ther Pat.2011;21:1831–41. https://doi.org/10.1517/13543776.2011.636354.
20. Guo ZH, Yin Y, Wang C, Wang PF, Zhang XT, Wang ZC, et al. synthesis and molecular docking of salicylic acid derivatives containing metronidazole as a new class of antimicrobial agents. Bioorg Med Chem. 2015;23:6148–56. https://doi.org/10.1016/j.bmc.2015.07.075.
21. Shchegol'kov EV, Shchur IV, Burgart YV, Saloutin VI, Trefilova AN, Ljushina GA, et al. Polyfluorinated salicylic acid derivatives as analogs of known drugs: Synthesis, molecular docking and biological evaluation. Bioorg Med Chem. 2017;25:91–9. https://doi.org/10.1016/j.bmc.2016.10.014.
22. Sharma H, Patil S, Sanchez TW, Neamati N, Schinazi RF, Buolamwini JK. Synthesis, biological evaluation and 3D-QSAR studies of 3-keto salicylic acid chalcones and related amides as novel HIV-1 integrase inhibitors. Bioorg Med Chem. 2011;19:2030–45. https://doi.org/10.1016/j.bmc.2011.01.047.
23. Ott I, Kircher B, Bagowski CP, Vlecken DHW, Ott EB, Will J, et al. Modulation of the biological properties of aspirin by formation of a bioorganometallic derivative. Angew Chem Int Ed. 2009;48:1160–3. https://doi.org/10.1002/anie.200803347.
24. Zielonka J, Joseph J, Sikora A, Hardy M, Ouari O, Vasquez-Vivar J, et al. Mitochondria-targeted triphenylphosphonium-based compounds: syntheses, mechanisms of action, and therapeutic and diagnostic applications. Chem Rev. 2017;117:10043–120. https://doi.org/10.1021/acs.chemrev.7b00042.
25. Reily C, Mitchell T, Chacko BK, Benavides GA, Murphy MP, Darley-Usmara VM. Mitochondrially targeted compounds and their impact on cellular bioenergetics. Redox Biol. 2013;1:86–93. https://doi.org/10.1016/j.redox.2012.11.009.
26. Fuentes-Retamal S, Sandoval-Acuña C, Peredo-Silva L, Guzmán-Rivera D, Pavani M, Torrealba N, et al. Complex mitochondrial dysfunction induced by TPP+-gentisic acid and mitochondrial translation inhibition by doxycycline evokes synergistic lethality in breast cancer cells. Cells. 2020;9:407–30. https://doi.org/10.3390/cells9020407.
27. Sandoval-Acuña C, Fuentes-Retamal S, Guzmán-Rivera D, Peredo-Silva L, Madrid-Rojas M, Rebolledo S, et al. Destabilization of mitochondrial functions as a target against breast cancer progression: role of TPP+-linked-polyhydroxybenzoates. Toxicol Appl Pharm. 2016;309:2–14. https://doi.org/10.1016/j.taap.2016.08.018.
28. Pugachev MV, Shtyrlin NV, Sysoeva LP, Nikitina EV, Abdullin TI, Iksanova AG, et al. Synthesis and antibacterial activity of novel phosphonium salts on the basis of pyridoxine. Bioorg Med Chem. 2013;21:4388–95. https://doi.org/10.1016/j.bmc.2013.04.051.
29. Tsepaeva OV, Nemtarev AV, Salikhova TI, Abdullin TI, Grigor'eva LR, Khozyainova SA, et al. Synthesis, anticancer and antibacterial activity of betulinic and betulonic acid C-28-triphenylphosphonium conjugates with variable alkyl linker length. Anticancer Agents Med Chem. 2020;20:286–300. https://doi.org/10.2174/1871520619666191014153554.
30. Tan W, Zhang J, Luan F, Wei L, Chen Y, Dong F, et al. Design, synthesis of novel chitosan derivatives bearing quaternary phosphonium salts and evaluation of antifungal activity. Int J Biol Macromol. 2017;102:704–11. https://doi.org/10.1016/j.ijbiomac.2017.04.073.
31. Tan W, Li Q, Wei L, Wang P, Gao Z, Chen Y, et al. Synthesis, characterization, and antifungal property of starch derivatives modified with quaternary phosphonium salts. Mater Sci Eng: C. 2017;76:1048–56. https://doi.org/10.1016/j.msec.2017.03.181.
32. Akhmadishina RA, Garifullin R, Petrova NV, Kamalov MI, Abdullin TI. Triphenylphosphonium moiety modulates proteolytic stability and potentiates neuroprotective activity of antioxidant tetrapeptides in vitro. Front Pharmacol. 2018;9:1–13. https://doi.org/10.3389/fphar.2018.00115.
33. Grymel M, Zawojak M, Adamek J. Triphenylphosphonium analogues of betulin and betulinic acid with biological activity: a

comprehensive review. J Nat Prod. 2019;82:1719–30. https://doi.org/10.1021/acs.jnatprod.8b00830.
34. Bittner Fialová S, Kello M, Čoma M, Slobodníková L, Drobná E, Holková I, et al. Derivatization of rosmarinic acid enhances its in vitro antitumor, antimicrobial and antiprotozoal properties. Molecules. 2019;24:1078–88. https://doi.org/10.3390/molecules24061078.
35. Tsepaeva O, Nemtarev A, Abdullin T, Grigoreva L, Kuznetsova E, Akhmadishina R, et al. Design, synthesis, and cancer cell growth inhibitory activity of triphenylphosphonium derivatives of the triterpenoid betulin. J Nat Prod. 2017;80:2232–39. https://doi.org/10.1021/acs.jnatprod.7b00105.
36. Garifullin R, Blokhin DS, Akhmadishina RA, Petrova NV, Kusova AM, Klochkov VV, et al. Effect of triphenylphosphonium moiety on spatial structure and biointeractions of stereochemical variants of YRFK motif. Eur Biophys J. 2019;48:25–34. https://doi.org/10.1007/s00249-018-1327-x.
37. Peredo-Silva L, Fuentes-Retamal S, Sandoval-Acuña C, Pavani M, Maya JD, Castro-Castillo V, et al. Derivatives of alkyl gallate triphenylphosphonium exhibit antitumor activity in a syngeneic murine model of mammary adenocarcinoma. Toxicol Appl Pharmacol. 2017;329:334–46. https://doi.org/10.1016/j.taap.2017.06.017.
38. Fueyo González FJ, Ebiloma GU, García CI, Bruggeman V, Sánchez Villamañán JM, Donachie A, et al. Conjugates of 2,4-dihydroxybenzoate and salicylhydroxamate and lipocations display potent antiparasite effects by efficiently targeting the trypanosoma brucei and trypanosoma congolense mitochondrion. J Med Chem. 2017;60:1509–22. https://doi.org/10.1021/acs.jmedchem.6b01740.
39. Ebiloma GU, Ayuga TD, Balogun EO, Gil LA, Donachie A, Kaiser M, et al. Inhibition of trypanosome alternative oxidase without its N-terminal mitochondrial targeting signal (ΔMTS-TAO) by cationic and non-cationic 4-hydroxybenzoate and 4-alkoxybenzaldehyde derivatives active against T. brucei and T. congolense. Eur J Med Chem. 2018;150:385–402. https://doi.org/10.1016/j.ejmech.2018.02.075.
40. Cortes LA, Castro L, Pesce B, Maya JD, Ferreira J, Castro-Castillo V, et al. Novel gallate triphenylphosphonium derivatives with potent antichagasic activity. PLoS ONE. 2015;10:e0136852 https://doi.org/10.1371/journal.pone.0136852.
41. Wodnicka A, Huzar E. Synthesis and photoprotective properties of new salicylic and vanillic acid derivatives. Curr Chem Lett. 2017;6:125–34. https://doi.org/10.5267/j.ccl.2017.3.002.
42. Smith RAJ, Hartley RC, Murphy MP. Mitochondria-targeted small molecule therapeutics and probes. Antioxid Redox Signal. 2011;15:3021–38. https://doi.org/10.1089/ars.2011.3969.
43. Manzano JI, Cueto-Diaz EJ, Olías-Molero AI, Perea A, Herraiz T, Torrado JJ, et al. Discovery and pharmacological studies of 4-hydroxyphenyl-derived phosphonium salts active in a mouse model of visceral leishmaniasis. J Med Chem. 2019;62:10664–75. https://doi.org/10.1021/acs.jmedchem.9b00998.
44. Jara JA, Castro-Castillo V, Saavedra-Olavarria J, Peredo L, Pavanni M, Jana F, et al. Antiproliferative and uncoupling effects of delocalized, lipophilic, cationic gallic acid derivatives on cancer cell lines. Validation in vivo in singenic mice. J Med Chem. 2014;57:2440–54. https://doi.org/10.1021/jm500174v.
45. Aykin-Burns N, Ahmad IM, Zhu Y, Oberley LW, Spitz DR. Increased levels of superoxide and H2O2 mediate the differential susceptibility of cancer cells versus normal cells to glucose deprivation. Biochem J. 2009;418:29–37. https://doi.org/10.1042/BJ20081258.
46. Plecitá-Hlavatá L, Ježek J, Ježek P. Pro-oxidant mitochondrial matrix-targeted ubiquinone MitoQ10 acts as anti-oxidant at retarded electron transport or proton pumping within Complex I. Int J Biochem Cell Biol. 2009;41:1697–707. https://doi.org/10.1016/j.biocel.2009.02.015.
47. Severin FF, Severina II, Antonenko YN, Rokitskaya TI, Cherepanov DA, Mokhova EN, et al. Penetrating cation/fatty acid anion pair as a mitochondria-targeted protonophore. PNAS. 2010;107:663–8. https://doi.org/10.1073/pnas.0910216107.
48. Fink BD, Herlein JA, Yorek MA, Fenner AM, Kerns RJ, Sivitz WI. Bioenergetic effects of mitochondrial-targeted coenzyme Q analogs in endothelial cells. J Pharmacol Exp Ther. 2012;342:709–19. https://doi.org/10.1124/jpet.112.195586.
49. Antonenko YN, Khailova LS, Knorre DA, Markova OV, Rokitskaya TI, Ilyasova TM, et al. Penetrating cations enhance uncoupling activity of anionic protonophores in mitochondria. PLoS ONE. 2013;8:e61902. https://doi.org/10.1371/journal.pone.0061902.g001.
50. Patková J, Anděl M, Trnka J. Palmitate-induced cell death and mitochondrial respiratory dysfunction in myoblasts are not prevented by mitochondria-targeted antioxidants. Cell Physiol Biochem. 2014;33:1439–51. https://doi.org/10.1159/000358709.
51. Trnka J, Elkalaf M, Anděl M. Lipophilic triphenylphosphonium cations inhibit mitochondrial electron transport chain and induce mitochondrial proton leak. PLoS ONE. 2015;10:e0121837. https://doi.org/10.1371/journal.pone.0121837.
52. Eruslanov E, Kusmartsev S. Identification of ROS using oxidized DCFDA and flow-cytometry, In: Armstrong D (eds.) Advanced protocols in oxidative stress II. Methods in Mol. Biol. 2010;594:57–72. https://doi.org/10.1007/978-1-60761-411-1_4.
53. Akhmadishina R, Kuznetsova E, Sadrieva G, Sabirzyanova L, Nizamov I, Akhmedova G, et al. Glutathione salts of O,O-diorganyl dithiophosphoric acids: Synthesis and study as redox modulating and antiproliferative compounds. Peptides. 2018;99:179–88. https://doi.org/10.1016/j.peptides.2017.10.002.
54. Valko M, Morris H, Cronin MT. Metals, toxicity and oxidative stress. Curr Med Chem. 2005;12:1161–208. https://doi.org/10.2174/0929867053764635.
55. Kamalov MI, Sadrieva GR, Pavlyuk AM, Salakhieva DV, Petrova NV, Abdullin TI. Synthesis and characterization of polyaspartic acid-histidine conjugate as an analog of antioxidant enzymes. Appl Biochem Microbiol. 2019;55:474–81. https://doi.org/10.1134/S0003683819050065.
56. Spivak AY, Nedopekina DA, Shakurova ER, Khalitova RR, Gubaidullin RR, Odinokov VN, et al. Synthesis of lupane triterpenoids with triphenylphosphonium substituents and studies of their antitumor activity. Russ Chem Bull. 2013;62:188–98. https://doi.org/10.1007/s11172-013-0028-y.
57. Millard M, Pathania D, Shabaik Y, Taheri L, Deng J, Neamati N. Preclinical evaluation of novel triphenylphosphonium salts with broad-spectrum activity. PLoS ONE. 2010;5:e13131. https://doi.org/10.1371/journal.pone.0013131.
58. Paterson DL. Resistance in gram-negative bacteria: enterobacteriaceae. Am J Infect Control. 2006;34:S20–8. https://doi.org/10.1016/j.ajic.2006.05.238.
59. Ma D, Cook DN, Hearst JE, Nikaido H. Efflux pumps and drug resistance in Gram-negative bacteria. Trends Microbiol. 1994;2:489–93. https://doi.org/10.1016/0966-842X(94)90654-8.
60. Dang T, Nizamov IS, Salikhov RZ, Sabirzyanova LR, Vorobev VV, Burganova TI, et al. Synthesis and characterization of pyridoxine, nicotine and nicotinamide salts of dithiophosphoric acids as antibacterial agents against resistant wound infection. Bioorg Med Chem. 2019;27:100–9. https://doi.org/10.1016/j.bmc.2018.11.017.
61. Galkina IV, Bakhtiyarova YV, Shulaeva MP, Pozdeev OK, Egorova SN, Cherkasov RA, et al. Synthesis and antimicrobial activity of carboxylate phosphabetaines derivatives with alkyl chains of various lengths. J. Chem. 2013:302937. https://doi.org/10.1155/2013/302937.
62. Kanazawa A, Ikeda T, Endo T. Synthesis and antimicrobial activity of dimethyl- and trimethyl-substituted phosphonium salts with alkyl chains of various lengths. Antimicrob Agents Chemother. 1994;38:945–52. https://doi.org/10.1128/AAC.38.5.945.